When habitat is lost matters: patterns of population decline and time to extinction in a seasonal, density-dependent model

Joseph B. Burant[1,2,*] and D. Ryan Norris[1]

Author affiliations:

[1] Department of Integrative Biology, University of Guelph, Guelph, Ontario, Canada, N1G 2W1

[2] Current address: Department of Animal Ecology, Netherlands Institute of Ecology, 6708 PB Wageningen, Netherlands

ORCID accounts:

JBB: https://orcid.org/0000-0002-0713-3100

DRN: https://orcid.org/0000-0003-4874-1425

* **Corresponding author**: j.burant@nioo.knaw.nl

Acknowledgements

This research was funded by a Discovery Grant to DRN from the Natural Sciences and Engineering Research Council of Canada. JBB was supported by an Ontario Graduate Scholarship and Queen Elizabeth II Graduate Scholarship in Science and Technology from the Ontario Government and a Graduate Tuition Scholarship from the University of Guelph.

Declarations

Funding: Natural Sciences and Engineering Research Council of Canada; Government of Ontario; University of Guelph

Conflicts of interest: The authors declare no competing interests.

Availability of data and material: The simulated data used in the analyses have been made available on Figshare: https://doi.org/10.6084/m9.figshare.14515194 (Burant and Norris 2023).

Code availability: The code for the theoretical model is publicly available on Figshare: https://doi.org/10.6084/m9.figshare.14515194 (Burant and Norris 2023).

Author contributions: Both authors were involved in initial discussions to develop the theoretical population model. JBB constructed the model, performed the analyses, and wrote the first draft. Both authors revised the manuscript for publication.

Ethics approval: Not applicable.

Consent to participate: Not applicable.

Consent to publication: Not applicable.

Manuscript summary:
Abstract word count: 254 words
Main text word count (excluding abstract, reference list, figure captions): 5,954 words
Number of figures: 5
Number of tables: 0
Number of references: 68
Number of supplementary items: 6

Abstract

Nearly all wild populations live in seasonal environments in which they experience regular fluctuations in environmental conditions that drive population dynamics. Recent empirical evidence from experimental populations of fruit flies suggests that demographic signals inherent in the counts of seasonal populations, including reproduction and survival, can indicate when in the annual cycle habitat loss occurred. However, it remains unclear whether these signatures of season-specific decline are detectable under a wider range conditions. Here, we use a bi-seasonal Ricker model previously developed and applied to the same experimental system to examine season-specific signals of population decline induced by different rates of habitat loss in the breeding or non-breeding season and different strengths of density dependence. Consistent with the findings in *Drosophila*, breeding habitat loss was accompanied by reduced reproductive output and a density-dependent increase in survival during the subsequent non-breeding period. Non-breeding habitat loss resulted in reduced non-breeding survival and a density-dependent increase in reproduction in the following breeding season. These season-specific demographic signals of decline were present under a wide range of habitat loss rates (2-25% per generation) and different density-dependent regimes (weak, moderate, and strong). We show that stronger density dependence can negatively influence time to extinction when non-breeding habitat is lost, whereas the strength of density dependence does not influence time to extinction with breeding habitat loss (although, in all cases, density dependence itself was an important modulator of population dynamics). Our results illustrate the need to incorporate seasonality in theoretical models to better understand when populations are being driven to decline.

Keywords: bi-seasonal, breeding, carrying capacity, density dependence, extinction, non-breeding, Ricker model, vital rates

Introduction

Habitat loss and fragmentation due to human land-use, have been identified as the leading causes of the dramatic declines in wild populations observed in recent decades (Pimm et al. 2014; Díaz et al. 2019; but see Fahrig 2003, 2019). Habitat deterioration is the primary risk to approximately 30 percent of threatened species and one of the major threats to 85 percent of all species identified on the IUCN's Red List (World Wildlife Fund 2018; Intergovernmental Science-Policy Platform on Biodiversity and Ecosystem Services 2019). An understanding of not only what environmental factors are driving these populations to extinction, but also when and where these forces play out within the annual cycle, is imperative to global conservation efforts. Simple demographic models provide a theoretical underpinning to our understanding of the dynamics of natural systems, and represent an important tool in our arsenal for characterizing, managing, and conserving threatened populations (Beissinger and Westphal 1998; Gimona 1999; Norris 2004; García-Díaz et al. 2019).

Climatic seasonality is a fundamental component of natural environments, driving the regular fluctuations in resource availability and quality to which most species and populations are subjected. And yet, early models of population growth, such as the logistic growth curve (Verhulst 1845; Pearl and Reed 1920) and the Ricker model (Ricker 1954) did not explicitly incorporate the potential for seasonal dependence, and the population dynamical implications of seasonality are generally underappreciated (White and Hastings 2020). Despite their simplicity, these models can still offer important insights into fundamental ecological processes that underpin the dynamics of a wide range of natural systems (Ricker 1963; Borlestean et al. 2015; Romero et al. 2017; Bolser et al. 2018). Although population models are still frequently framed around a stationary, or 'aseasonal', context (Ludwig 1996; Mueller and Joshi 2000; Lande et al. 2003; Otso and Meerson 2010), explicit incorporation of the impacts of seasonality on population dynamics has proven fruitful (Skellam 1967; Fretwell 1972; Kot and Schaffer 1984; Sutherland 1996; Norris 2005; Liz 2017).

Despite lacking explicit seasonality, the strength of simple population models like the logistic and Ricker models is that they capture the important role of density dependence in explaining fluctuations in abundance over time. Density-dependent mechanisms arise when the rate of population growth at any given time is, at least in part, contingent on the current population density (Hassell 1986). The strength of density dependence is expected to modulate

the effects of habitat loss and impact population responses to environmental change (Sutherland 1996; Agrawal et al. 2004; Norris 2005). Sequential density dependence, through which population abundance in one season influences population vital rates in the next (Norris 2005; Ratikainen et al. 2007; Betini et al. 2013a), may affect the capacity for populations to respond to environmental change, and may also result in different system dynamics in those losing breeding or non-breeding habitat. In a series of studies, Betini et al. (2013a, 2013b, 2014) demonstrated how density dependence acts to regulate seasonal population dynamics in an experimental population of *Drosophila melanogaster* with distinct breeding and non-breeding periods.

In a recent experimental study, we investigated how seasonal changes in habitat availability influenced the dynamics of the same seasonal *Drosophila* populations, and found that populations losing breeding versus non-breeding habitat responded in the different ways (Burant et al. 2019). In the experiment, seasonality was induced by manipulating the quality food provided (Betini et al. 2013b) and chronic, season-specific habitat loss was imposed over multiple generations by systematically reducing the volume of food provide in one period while holding it constant in the other (Burant et al. 2021). The loss of breeding habitat resulted in a decline in *per capita* reproduction and, as a consequence of fewer individuals entering the subsequent non-breeding period, a positive density-dependent increase in non-breeding survival. Conversely, non-breeding habitat loss had the opposite effects: non-breeding survival declined due to resource limitation, while *per capita* reproduction showed a density-dependent increase in the subsequent breeding period (Burant et al. 2019). Moreover, we demonstrated that simple demographic and statistical signals derived from population counts and vital rates, including non-breeding survival, reproduction and other statistical indicators inherent in time series of population abundance, can be used to identify the season in which habitat loss occurred (Burant et al. 2019). However, the experiment only considered two different rates of breeding or non-breeding habitat loss (10% and 20% per generation) and was conducted under levels of breeding and non-breeding density dependence characteristic of a specific, laboratory-evolved strain of *Drosophila*. Thus, the extent to which these empirical results are relevant for other populations under a broader range of strengths of density dependence and rates of habitat loss remains unclear.

In this study, we use a bi-seasonal Ricker model (Betini et al. 2013a) to explore how different rates of habitat loss in either the breeding or non-breeding period and the strength

density dependence influence the production of simple, season-specific signals of population decline and time to extinction *in silico*. The original (aseasonal) Ricker model was developed in the context of fisheries harvesting (Ricker 1954) and has since been extended for application in a variety of contexts, modelling the population dynamics for a broad range of taxa, including fishes (e.g., Myers et al. 1999), crustaceans (e.g., Twombly et al. 2007), and insects (e.g., Dey and Joshi 2006; Estay et al. 2009). Here, we incorporate the effects of season-specific habitat loss on carrying capacity and growth in each period of the bi-seasonal model, and use simulations to explore how habitat loss operates under a range of initial parameter values, strengths of density dependence, and rates of seasonal habitat loss. We derive season-specific vital rates (survival and reproduction) to look at sequential density-dependence between periods of breeding and non-breeding (Betini et al. 2013a), rather than density dependence in population growth between generations.

Given the discrete nature of our model, with breeding and non-breeding conditions modelled as two separate equations and resource pools (habitats), we expect that this model may be particularly relevant for migratory species (e.g., migratory birds) that occupy distinct breeding and non-breeding habitats. For example, our model captures the plausible scenario in which a population experiences habitat loss (or other environmental forcing) on the breeding grounds, while the non-breeding sites remain relatively stable (or *vice versa*). However, even in resident species that occupy the same habitat throughout the year, populations may experience differential changes in resource availability and quality during periods of breeding and non-breeding, which may similarly impact their overall dynamics. Thus, the model we present and others that explicitly incorporate seasonality (White and Hastings 2020) have a broad scope of application.

Methods

Bi-seasonal Ricker model with season-specific habitat loss

The Ricker model (eq. 1) was first introduced by W.E. Ricker (1954) in the context of fisheries management, following his observation that the convex relationship between net reproduction and population density resulted in oscillations in population abundance. Since then, the Ricker model has become one of the classical theoretic models to describe density-dependent dynamics

in populations with discrete time intervals (Fretwell 1972; Kot and Schaffer 1984; Turchin 2003; Geritz and Kisdi 2004; Wysham and Hastings 2008). The Ricker model can be expressed as:

$$N_{(t+1)} = N_{(t)} e^{r\left(1-\frac{N_{(t)}}{K}\right)} \quad \text{(eq. 1)}$$

where N represents the number of individuals in the population at a given time t, r is the intrinsic growth rate ('Malthusian parameter'; Fisher 1930), and K indicates a population's carrying capacity (Pearl and Reed 1920). The simple Ricker model has been used previously to model the population dynamics of *Drosophila* (Mueller and Joshi 2000; Dey and Joshi 2006). This aseasonal model results in stable population cycles for a range of r and K, which can be either arbitrary or empirically defined, but generates chaotic dynamics when r is large (r > ~2.7; May and Oster 1976; May 1987). Griffen and Drake (2008) showed that reductions in habitat quality produced reductions in both r and K, as modelled for experimental populations of the water flea *Daphnia magna*.

To investigate the dynamics of *D. melanogaster* with distinct breeding and non-breeding periods, Betini et al. (2013a) extended the Ricker model to include season-specific parameters for population growth and carry capacity. For this 'seasonal' Ricker model, temporal changes in breeding (N_b) and non-breeding (N_{nb}) population abundance can be modelled using a set of two interacting equations (eq. 2.1, 2.2). For each generation, population size at the beginning of the non-breeding period (i.e., the number of offspring produced; maximum population size in a given generation) can be written as the difference equation:

$$N_{nb(t+1)} = N_{b(t)} e^{r_b\left(1-\frac{N_{b(t)}}{K_b}\right)} \quad \text{(eq. 2.1)}$$

where r_b and K_b are the maximum growth rate (reproduction) and carrying capacity for the breeding period, b, respectively. In this way, nonbreeding, nb, population size (N_{nb}) is a product of the number of breeders (N_b) and density-dependent interactions between them (Betini et al. 2013a, 2013b). Population size at the beginning of the breeding period (i.e., the number of potentially breeding adults that survived the previous non-breeding period) can be described as:

$$N_{b(t+1)} = N_{nb(t+1)} e^{r_{nb}\left(1-\frac{N_{nb(t+1)}}{K_{nb}}\right)} \quad \text{(eq. 2.2)}$$

where r_{nb} and K_{nb} are the maximum growth rate (mortality) and carrying capacity for the non-breeding period, respectively.

In this study, we were interested in modelling the impacts of chronic, season-specific habitat loss on the predicted changes in breeding and non-breeding population size under a range of conditions. In a previous experiment (Burant et al. 2019), we systemically reduced the amount of food provided to replicate populations of *Drosophila* in either the breeding or non-breeding period over multiple generations, until the populations went extinct. In our experiment, and in the theoretical model presented here, season-specific habitat loss followed an exponential decay, with the proportion of food provisioned in the season of habitat loss in a particular generation $H_{(t)}$ prescribed as:

$$H_{(t)} = (1 - v)^t \quad \text{(eq. 3)}$$

*w*here v is the rate of habitat loss and *t* is the number of generations since habitat loss treatment commenced.

In an attempt to replicate the experimental reductions in habitat, we represented habitat loss by altering season-specific *r* and *K* parameters. Given that both population growth rate and carrying capacity have been shown to be dependent on the quantity of food provisioned (Griffen and Drake 2008), we scaled both parameter values proportionally with the rate of habitat loss. For populations losing breeding habitat, our model assumed that both r_b and K_b would decrease proportionally with the rate of habitat loss (eq. 4.1), such that the total number of offspring produced by the previous generation $N_{nb(t+1)}$ would also decrease. Changes in population growth rates and carrying capacities with breeding habitat loss can be summarized as:

$$K_{b(t)} = K_b^* H_{b(t)} \quad \text{(eq. 4.1)}$$

$$r_{b(t)} = r_b^* - r_b^*\left(1 - H_{b(t)}\right) = r_b^* H_{b(t)}$$

$$K_{nb(t)} = K_{nb}^*$$

$$r_{nb(t)} = r_{nb}^*$$

where K_b^* and r_b^* are the estimated carrying capacity and intrinsic growth rate during the breeding period under control (no habitat loss) conditions, respectively, K_{nb}^* and r_{nb}^* are the corresponding non-breeding values, and $H_{b(t)}$ is the proportion of breeding habitat remaining.

For populations losing non-breeding habitat, we expected the opposite effects on season-specific growth rates and carrying capacities. We predicted that K_{nb} would decrease proportionally to the rate of habitat loss and r_{nb} would become more negative (increasing

mortality) as the proportion of habitat remaining continued to decline (eq. 4.2). Changes in population growth rates and carrying capacities with non-breeding habitat loss can be summarized as:

$$K_{b(t)} = K_b^* \qquad \text{(eq. 4.2)}$$

$$r_{b(t)} = r_b^*$$

$$K_{nb(t)} = K_{nb}^* H_{nb(t)}$$

$$r_{nb(t)} = r_{nb}^* - |r_{nb}^*|\left(1 - H_{nb(t)}\right)$$

where $H_{nb(t)}$ is the proportion of non-breeding habitat remaining. Scaling the season-specific growth rates and carrying capacities in this way had the effect of holding the strength of density dependence (see below) constant in the season of habitat loss.

Theoretical model simulations

To explore the dynamics of our bi-seasonal Ricker model with season-specific habitat loss, we first parameterized the model using estimates derived from a set of input-output experiments in seasonal populations of *Drosophila* (Betini et al. 2013a). In these trials, populations of breeding and non-breeding fruit flies were initiated at a range of densities, and their subsequent reproductive output (breeding) and survival (non-breeding) were measured. The experimental density dependence reference parameters from Betini et al. (2013a) were: $r_b = 2.24$, $\alpha_b = 9.86 \times 10^{-3}$, $r_{nb} = -0.0568$, and $\alpha_{nb} = 6.72 \times 10^{-4}$, where α describes the strength of density dependence in an alternative form of the Ricker model and can be calculated as $\alpha_i = r_i / K_i$ (see *Supplementary Information* for results of model parameterization with empirical values; Fig. S3).

To investigate how the strength of density dependence influenced the trajectories of populations and the production of seasonal signals of decline, we further explored three other parameterizations in which the strength of density dependence was manipulated by changing the value of r (in the same direction) in both seasons: (1) weak density dependence ($r_b = 1.3$, $r_{nb} = -0.033$); moderate density dependence ($r_b = 2$, $r_{nb} = -0.051$); strong density dependence ($r_b = 2.65$, $r_{nb} = -0.069$). These values of r_b are selected somewhat arbitrarily to sample the range of the non-zero equilibrium, non-chaotic phase of the Ricker model ($r < 1$ results in populations shrinking to zero; chaotic dynamics set in at $r \approx 2.7$). The corresponding r_{nb} values are matched based on

the ratio of the experimentally-derived parameters (e.g., $r_{nb(moderate)} = r_{nb(experimental)}$ x 2 / 2.24). This manipulation of r is consistent with previous experimental work, which has shown that, intuitively, maximum growth rates may be useful as a predictor of the strength of density dependence in systems that conform to the monotonic definition of density dependence inherent in most simple population models (Agrawal et al. 2004). Because carrying capacity is largely a function of the volume of food provided (e.g., Griffen and Blake 2018; Burant et al. 2020), and not the strength of density dependence, the season-specific carrying capacities (K_b = 227, K_{nb} = -84.5) were the same for all three theoretical scenarios and the initial empirical parameterization.

To simulate some degree of variability in the baseline parameters, which should be expected for real world replicate populations, we treated these parameters as normal distributions $N(\mu, \sigma^2)$ from which the initial values K_b^*, r_b^*, K_{nb}^*, and r_{nb}^* could be sampled. For the season-specific carrying capacities, the standard deviation of K_i was set as $\sqrt{|K_i|}$. Since the square-root of a value < 1 is larger than the initial value, the standard deviation for the season-specific growth rates r_i was set as r_i /10.

We simulated a range of rates of season-specific habitat loss, with populations losing habitat at a rate of 2%, 5%, 10%, 20%, or 25% per generation in either the breeding or the non-breeding period. We also included control simulations, in which habitat availability was constant in both seasons. As with our experiment, which included 10% and 20% rates of habitat loss (Burant et al. 2019), replicate simulations were initiated with a non-breeding population size of 20 individuals. We simulated 20 generations of 'pre-treatment' population growth in which the proportion of habitat provisioned in the treatment period remained at 100%. Starting in generation 21, the simulated proportion of habitat provisioned in the treatment period corresponded to the rate of loss following eq. 3. We ran each model simulation for 50 generations (including the pre-treatment period), or until the population went extinct.

For each strength of density dependence scenario, we performed 1,000 model simulations for different rate of loss and season of loss combinations (e.g., 2% breeding, 2% non-breeding, 5% breeding, etc.), with 10 rate-by-season treatment combinations plus controls. In order to avoid overfitting our statistical models (see *Supplementary Information*), and to introduce an additional degree of randomness in the initial parameter values that were used to specify each run, we randomly sampled 25 of the 1,000 simulations for each treatment for analysis.

From each replicate, we derived time series of the following metrics: (1) *breeding abundance* (i.e., the number of potential breeders, the number of individuals at the end of the non-breeding period); (2) *non-breeding abundance* (i.e., the number of offspring produced, the number of individuals at the start of the non-breeding period); (3) *per capita reproduction* (i.e., the relative change in abundance between the beginning and end of the breeding period, non-breeding abundance / breeding abundance); and (4) *non-breeding survival* (i.e., the relative change in abundance between the beginning and end of the non-breeding period, breeding abundance / non-breeding abundance). Time to extinction was calculated as the number of generations from the initiation of habitat loss (i.e., generation – 20) until abundance ≤ 2 individuals in the breeding period.

Relative strength of density dependence

To explore the density-dependent nature of time to extinction that we identified in our model simulations of non-breeding habitat loss, we systemically varied the strength of density dependence in either the breeding and non-breeding period independently while holding density dependence constant (moderate) in the other season. As with all parameterizations, the relative strength of density dependence was always higher in the breeding period ($\alpha_{weak} = 5.73 \times 10^{-3}$, $\alpha_{moderate} = 8.81 \times 10^{-3}$, $\alpha_{strong} = 1.17 \times 10^{-2}$) than that in non-breeding period ($\alpha_{weak} = 3.91 \times 10^{-4}$, $\alpha_{moderate} = 6.00 \times 10^{-4}$, $\alpha_{strong} = 8.11 \times 10^{-4}$; see *Theoretical model simulations*). Extinction time was determined by performing a single iteration of the non-breeding habitat loss model with each combination of breeding and non-breeding strengths of density dependence.

The theoretical model was constructed in the R statistical environment (v. 4.0.2; R Core Team 2020). The code and data used in these analyses have been made publicly available (Burant and Norris 2022).

Results

Bi-seasonal population dynamics with habitat loss

Simulations of a bi-seasonal Ricker model with season-specific habitat loss (see *Theoretical model simulations* in *Methods*) produced two counts in each generation (breeding abundance and non-breeding abundance), with distinct dynamics that varied with the season and rate of habitat

loss (Fig. 1). In the initial pre-treatment generations, during which all replicate populations were allowed to grow from an initial non-breeding population size of 20 individuals, all treatment scenarios showed a rapid increase towards carrying capacity and stable seasonal oscillations in the generations preceding the introduction of treatment. For control replicates, in which habitat availability remained constant in both the breeding and non-breeding period, population abundances in both seasons were stable throughout the treatment period. Control breeding abundance was largely similar across the different strengths of density dependence (mean breeding abundance: weak DD = 206 ± 2.48 (mean ± SE); moderate DD = 200 ± 3.89; strong DD = 199 ± 2.51; Fig 1a; Fig. S1). In contrast, control non-breeding abundance increased with the strength of density dependence (mean non-breeding abundance: weak DD = 233 ± 3.20; moderate DD = 247 ± 5.54; strong DD = 276 ± 26.5; Fig. 1a; Fig. S2). Between-season variability in abundances increased with stronger density dependence (Fig. 1).

With reductions in breeding habitat, there were similar patterns of decline in both breeding and non-breeding abundance, with declines in both seasons beginning within 1-2 generations of the onset of treatment (Fig. 1b; Fig. S1; Fig. S2). In contrast, when non-breeding habitat was lost, breeding and non-breeding population abundance appeared to diverge in simulations (Fig. 1c; Fig. S1; Fig. S2). Breeding population abundance declined steadily as non-breeding habitat was lost, whereas non-breeding population abundance remained relatively stable for several generations before declining rapidly. At lower rates of non-breeding habitat loss (2% and 5% per generation), non-breeding abundance actually increased slightly for several generations preceding the rapid decline (Fig. 1b; Fig. S2). The transition from high, stable non-breeding abundance to rapid decline occurs around generation 21, 16, 14, 12, and 11 for non-breeding habitat loss treatments of 2%, 5%, 10%, 20%, and 25% habitat loss per generation (Fig. S3).

Response of vital rates to season-specific habitat loss

As expected, breeding and non-breeding habitat loss generated distinct changes in population vital rates (Fig. 2; Fig. 3; *Supplementary Information*). For control replicates, *per capita* reproduction declined rapidly as populations grew towards carrying capacity in the pre-treatment period, and remained stable during the treatment generations (mean *per capita* reproduction = 1.13 ± 0.004, 1.28 ± 0.04, and 2.07 ± 0.40 offspring/breeder with weak, moderate, and strong

density dependence, respectively; Fig. 2a). When breeding habitat was lost, *per capita* reproduction dropped and remained below one (i.e., the replacement value) as the amount of breeding habitat available in each generation continued to decline. *Per capita* reproduction shifted from being relatively stable in the generations preceding population collapse to zero within a single generation (Fig. 2b). In contrast, non-breeding habitat loss generated a steady increase in *per capita* reproduction, with values exceeding those observed for control simulations, as one might expect given the assumed pattern of compensatory density dependence (Fig. 2c). As the rate of non-breeding habitat loss increased, the relative increase in *per capita* reproduction decreased, likely as a result of reduced time available for simulations to respond to shifting conditions.

Non-breeding survival remained relatively high throughout the treatment period for control simulations (mean non-breeding survival = 88.4 ± 0.003%, 79.1 ± 0.006%, and 75.7 ± 0.02% for weak, moderate, and strong density dependence, respectively), and was as high as 100% in the initial generations of the pre-treatment period (Fig. 3a). When breeding habitat was lost, the proportion of individuals that survived the non-breeding period increased to one as the number of individuals entering the non-breeding period decreased (Fig. 3b). With non-breeding habitat loss, non-breeding survival decreased proportionally with the rate of habitat loss (Fig. 3c). Interestingly, all non-breeding habitat loss simulations reached a plateau around 20-25% non-breeding survival in later generations (i.e., when the volume of non-breeding habitat provisioned was low), with non-breeding survival actually increasing in the generation preceding population collapse, before declining to zero as the populations went extinct. This result may provide some evidence for an Allee effect on survival with non-breeding habitat loss, likely because relatively few offspring are produced by breeders at very low densities.

Time to extinction

Season-specific habitat loss resulted in rapid changes in bi-seasonal population dynamics, with breeding and non-breeding habitat loss generating different patterns of population decline and timing of population collapse (Fig. 1b, c). As expected, the pace at which populations declined towards extinction increased with the rate of habitat loss. However, there was a notable difference between simulations of breeding and non-breeding habitat loss in the effect of the strength of density dependence on the timing of population collapse (Fig. 4). When breeding

habitat was lost, the timing of population collapse appeared to be almost entirely dependent on the rate of habitat loss, with relatively little impact of the strength of density dependence imposed on the population (Fig. 4a). With breeding habitat loss, all replicate populations went extinct within 19, 11, 7, 4, and 3 generations with the onset of habitat loss treatments of 2%, 5%, 10%, 20%, and 25% loss per generation, respectively. In contrast, when non-breeding habitat was lost, the time to extinction was negatively related to the strength of density dependence (Fig. 4b), such that populations subjected to weak density dependence collapsed later than those subjected to strong density dependence. Across all scenarios, populations losing non-breeding habitat went extinct earlier than those losing breeding habitat (Fig. 1; Fig. 4; Fig. S3).

Because we varied the strength of density dependence simultaneously in both seasons, we were also interested in examining whether season-specific variation in density dependence could be driving the negative relationship between density dependence and time to extinction when non-breeding habitat was lost. To do this, for the non-breeding habitat loss scenarios, we varied the strength of density dependence in one period while holding the other at a moderate level, and then examined the time to extinction. When the strength of non-breeding density dependence was held at a moderate level and non-breeding habitat was lost, stronger breeding density dependence resulted in earlier population extinction (Fig. 5a), similar to the results reported above. In contrast, when breeding density dependence was held at a moderate level and non-breeding habitat was lost, variation in the strength of non-breeding density dependence had no impact on the timing of population collapse (Fig. 5b).

Discussion

We were interested in exploring whether a simple phenomenological model could be used to capture and extend the dynamics observed in experimental populations exposed to chronic, season-specific habitat loss. In our previous experiment, we showed that when and where habitat was lost had important consequences for the way in which populations decline, and had unique effects on seasonal vital rates (Burant et al. 2019). Several broad similarities in the overall patterns of decline from our experiment and theoretical model suggest that the latter does a reasonable job of approximating the former. First, while mean extinction times estimated from the model (see *Bi-seasonal population dynamics with habitat loss* in *Results*) were earlier than experimentally-induced collapses (average times to extinction with 10% and 20% habitat loss per

generation were 14 and 7 generations for breeding treatments, and 14 and 8 generations for non-breeding treatments; Burant et al. 2019), the relative order in extinction of populations losing breeding and non-breeding habitat was consistent with experimental observations. Likewise, in both the experiment and the model presented here, non-breeding habitat loss produced large fluctuations between breeding and non-breeding population abundance (as a result of density-dependent reproduction), while breeding habitat loss resulted in consistent, directional decline (compare Fig. 1 herein with Figure 2 in Burant et al. (2019)).

Our theoretical results demonstrate the important role that the strength of density dependence plays in determining how populations decline with seasonal habitat loss. Based on our simulations, the timing of population collapse with habitat deterioration during the breeding period was almost entirely dependent on the rate at which habitat was lost, with no impact of changes in the strength of density dependence. In contrast, strong density dependence amplified the impacts of non-breeding habitat loss, such that increased density dependence resulted in steeper population declines and earlier extinctions. The difference in the influence of density dependence with season-specific habitat loss is consistent with our predictions, and is ultimately a reflection of differences in the capacity of populations to respond to habitat loss in either the breeding or non-breeding period. With non-breeding habitat loss, populations may experience a 'seasonal compensation effect' (Norris 2005) that results in increased reproduction in the subsequent breeding period. A similar compensatory effect should not necessarily be expected with breeding habitat loss, since, by definition, populations cannot grow during the subsequent non-breeding period. Moreover, any seasonal compensation effect with breeding habitat loss is constrained by ceiling effects, since the proportion of individuals that survive the non-breeding period cannot exceed 100 percent. This conclusion was supported by an exploratory analysis in which we manipulated the strength of density dependence separately in each period, which showed that changing non-breeding density dependence did not affect time to extinction when breeding density dependence was moderate.

Inspection of the breeding and non-breeding population abundance time series revealed a number of important differences between our theoretical and experimental results (see *Supplementary Information*). First, while the relative (but not absolute) timing of collapse was consistent between the experiment and model (see above), the way in which these declines unfolded differed. Although experimental populations did not appear to respond immediately to

breeding habitat loss, with population size remaining relatively stable for several generations before declining precipitously (largely due to stable breeding abundances resulting from the strong filter of the non-breeding period; Burant et al. 2019), our theoretical model generated steady declines in abundance in both seasons with the onset of breeding habitat loss. Non-breeding habitat loss had similar effects on seasonal abundances, with delayed declines in non-breeding population size relative to breeding (as a result of density-dependent reproduction; Burant et al. 2019). Despite the fact that the control conditions in the experimental seasonal *Drosophila* system were empirically derived (G.S. Betini and D.R. Norris, *unpublished data*), it is possible that initial breeding food availability in our experiments was in excess of what was required to maintain stable bi-seasonal dynamics. This could have resulted in a delayed population response to reductions in breeding habitat. Moreover, carrying capacity in either season is not solely a function of the volume of food provided, since there is only so much space the flies can occupy in a closed system, and so there is the potential for overcrowding (rather than absolute food availability) to limit food access and ultimately affect differences in survival and reproduction (Burant et al. 2020; Kilgour et al. 2020). The potential for overcrowding was not accounted for in our theoretical model, and so changes in carrying capacity were assumed to be simply a function of food availability (see *Bi-seasonal Ricker model with season-specific habitat loss* in *Methods*). As a consequence of these intricacies, relative to our experiment (Burant et al. 2019), the simple theoretical model generally underestimated breeding and non-breeding population abundance with breeding habitat loss, and overestimated breeding abundance when non-breeding habitat was lost.

We noted that, for non-breeding habitat loss simulations, non-breeding survival appeared to temporarily plateau in later generations when little non-breeding habitat remains and, in some instances, briefly increased in the generation preceding extinction (Fig. 3c). While not specifically encoded in the model, this is reminiscent of an Allee effect (Allee 1927; Stephens et al. 1999) in which population growth is limited at low breeding densities. In essence, low non-breeding habitat availability means only a few individuals survive to the next breeding period and, as a result, reproductive output and population growth are reduced due to low densities. In turn, only a few individuals enter the subsequent non-breeding period, where habitat availability continues to decline. Thus, non-breeding densities may be better matched to habitat availability than in previous generations when non-breeding survival declined rapidly due to the breeding

season density-dependent, rebound-induced mismatch between the number of individuals entering the non-breeding period and the declining habitat availability. This plateau means populations persist longer than might otherwise be anticipated based on the steep decline in non-breeding survival observed at earlier timepoints. Why this arises in our model is not necessarily intuitive, but is possibly a product of the interplay between the density-dependent r_b (stable) and r_{nb} (increasingly negative). Allee effects have been explicitly incorporated in other modifications of the Ricker model (Elaydi and Sacker 2009), including the periodic Ricker map (Sacker 2006).

There are several other potential explanations for discrepancies between our previous observational results and theoretical outcomes. Betini et al. (2013a) showed that sequential density dependence and carry-over effects between seasons can influence reproductive output and regulate population abundance. However, fluctuations in population density and food availability between seasons are also expected to influence other aspects of individual and population performance, which may help to buffer populations against deteriorating environmental conditions. For example, reproductive output is known to be influenced by individual body condition, such that individuals who enter the breeding period in poor condition produce fewer offspring (Betini et al. 2014), and non-breeding food availability carries over to indirectly influence reproductive performance (Burant et al. 2020). These phenotypic traits, and their changes in response to seasonal variation, effectively link environmental conditions in one season with individual performance in the next (O'Connor et al. 2014). Similarly, intraspecific interactions among individuals in a population can be density-mediated, with individual behavioural expression modulated by the social context (Sokolowski et al. 1997; Kilgour et al. 2018; Leatherbury and Travis 2019). Importantly, the impacts of density-dependent changes on population growth and individual traits are not necessarily immediately observable (Ratikainen et al. 2007). These are but a few examples of the mechanisms through which individuals and populations can respond to changing environmental conditions (Colchero et al. 2018). Although the purpose of simple population models is not necessarily to reproduce all possible mechanisms of change, discrepancies between our theoretical and empirical results demonstrate the importance of considering carry-over effects and other non-abundance traits that are expected to shift as the environment deteriorates. Indeed, recent theoretical work has demonstrated the importance of considering the impacts of seasonal carry-over effects on individual performance and, ultimately, how these effects scale up to influence population vital rates (e.g., Liz and Ruiz-

Herrera 2016). Failure to fully consider carry-over effects is likely to limit our understanding of the dynamics of declining populations, and so also limit efforts to conserve them (O'Connor and Cooke 2015).

The present model is not the first to consider how seasonality shapes the dynamics of animal populations. Fretwell (1972) expounded at length about the various ways regularly varying environments influences individual reproduction and survival and, ultimately, population persistence. Others have considered the more general case of resource variability across different temporal scales (e.g., Hastings 2014). In its original formulation, the bi-seasonal Ricker model from Betini et al. (2013a) was important for demonstrating how explicit incorporation of density-mediated carry-over effects better captures long-term vital rate dynamics and population stability. The interplay between seasonality and stability was also explored by Kot and Schaffer (1984), who showed theoretically how moderate seasonality may stabilize populations in productive environments. Consistent with our findings, Kot and Schaffer (1984) also showed how increasing 'imbalance' between breeding and non-breeding seasons periods can have contrasting effects. Sutherland (1996) more explicitly considered the effects of season-specific habitat loss on the dynamics of migratory populations, and similarly found differential effects of breeding and non-breeding habitat loss. Although time to extinction was not directly evaluated, Sutherland (1996) showed that, compared to breeding habitat loss, the same amount of non-breeding habitat loss had more than twice the effect in terms of percent population decline. This is consistent with our finding that populations losing non-breeding habitat go extinct earlier than those losing breeding habitat. Our analysis complements these previous studies by showing how sequential density-dependent effects can modulate patterns of population decline and time to extinction with chronic, season-specific forcing. By simulating habitat deterioration in one season and holding it fixed in the other, we begin to explore how seasonal populations may be temporarily buffered against decline through density-dependent survival and reproduction. Finally, while we implement a seasonal formulation of the Ricker model, many other simple demographic models exist and predictions from these models may differ from those presented here. Previous comparison of the utility of different aseasonal models for predicting extinction in a community context has shown that the strong density dependence inherent in the Ricker model best matched results from simple microcosms (Ferguson and Ponciano 2013).

Along with understanding the demographic mechanisms underlying patterns of population decline, it is relevant to consider whether the predictability of collapse differs between populations losing breeding and non-breeding habitat. In our chronic habitat loss experiment, we showed that whether a set of indicators derived from time series of population abundance (e.g., coefficient of variation, lag-1 autocorrelation) and fitness-related traits (e.g., body size, activity) served as early warning indicators of population collapse was dependent on the season of habitat loss (Burant et al. 2021). Moreover, in a similar theoretical approach to the one presented here, Bury (2020) showed that the nature of early warning signal production differed between simulations of breeding and non-breeding habitat degradation. This theoretical work also suggests the potential for using early warning indicators to identify the season in which populations are being driving to decline, which we also previously demonstrated in our experimental system (Burant et al. 2019). These results suggest that simple demographic vital rates like survival and reproduction, as well as early warning indicators, may be useful for detecting and predicting season-specific drivers of population decline across a wide range of density-dependent systems.

In summary, the results from our theoretical model of the impacts of season-specific habitat loss on population dynamics through changes in growth and carrying capacity bolster our understanding of how populations decline in seasonal environments. By comparing our theoretical simulations to results from an earlier chronic habitat loss experiment, we are able to identify some of the ways in which simple population models can elegantly capture real-world phenomena. Along with experiments and observational studies, theoretical models represent an important tool, not only for understanding how the natural world works but particularly for efforts aimed at conserving threatened species in an era of rapid environmental change.

References

Agrawal AA, Underwood N, Stinchcombe JR (2004) Intraspecific variation in the strength of density dependence in aphid populations. Ecol Entomol 29:521-526. https://doi.org/10.1111/j.0307-6946.2004.00635.x

Allee WC (1927) Animal aggregations. Quart Rev Biol 2:367-398. https://doi.org/10.1086/394281

Beissinger SR, Westphal MI (1998) On the use of demographic models of population viability in endangered species management. J Wildl Manage 62:821-841. https://doi.org/10.2307/3802534

Betini GS, Griswold CK, Norris DR (2013a) Carry-over effects, sequential density dependence and the dynamics of populations in a seasonal environment. Proc R Soc Lond B 280:20130110. https://doi.org/10.1098/rspb.2013.0110

Betini GS, Griswold CK, Norris DR (2013b) Density-mediated carry-over effects explain variation in breeding output across time in a seasonal population. Biol Lett 9:20130582. https://doi.org/10.1098/rsbl.2013.0582

Betini GS, Griswold CK, Prodan L, Norris, DR (2014) Body size, carry-over effects and survival in seasonal environment: consequences for population dynamics. J Anim Ecol 3:1313-1321. https://doi.org/10.1111/1365-2656.12225

Bolser DG, Grüss A, Lopez MA, Reed EM, Mascareñas-Osorio I, Erisman BE (2018) The influence of sample distribution on growth model output for a highly exploited marine fish, the Gulf corvina (*Cynoscion othonopterus*). PeerJ 6:e5582. https://doi.org/10.7717/peerj.5582

Borlestean A, Frost PC, Murray DL (2015) A mechanistic analysis of density dependence in algal population dynamics. Front Ecol Evol 3:37. https://doi.org/10.3389/fevo.2015.00037

Burant JB, Betini GS, Norris DR (2019) Simple signals indicate which period of the annual cycle drives declines in seasonal populations. Ecol Lett 22:2141-2150. https://doi.org/10.1111/ele.13393

Burant JB, Griffin A, Betini GS, Norris DR (2020). An experimental test of the ecological mechanisms driving density-mediated carry-over effects in a seasonal population. Can J Zool 96:425-432. https://doi.org/10.1139/cjz-2019-0271

550 Burant JB, Norris, DR (2023) Code and data from: When habitat is lost matters: patterns of
551 population decline and time to extinction in a seasonal, density-dependent model. Figshare.
552 https://doi.org/10.6084/m9.figshare.14515194
553 Burant JB, Park C, Betini GS, Norris DR (2021) Early warning indicators of population collapse
554 in a seasonal environment. J Anim Ecol 90:1538-1549. https://doi.org/10.1111/1365-
555 2656.13474
556 Bury T (2020) Detecting and distinguishing transitions in ecological systems: model and data-
557 driven approaches. Dissertation, University of Waterloo, Waterloo
558 Carpenter B, Gelman A, Hoffman MD, Lee D, Goodrich B, Betancourt M, Brubaker M, Guo J,
559 Li P, Riddell A (2017) Stan: a probabilistic programming language. J Stat Softw 76:1-29.
560 https://doi.org/10.18637/jss.v076.i01
561 Colchero F, Jones OR, Conde DA, Hodgson D, Zajitschek F, Schmidt BR, Malo AF, Alberts SC,
562 Becker PH, Bouwhuis S, Bronikowski AM, De Vleeschouwer KM, Delahay RJ,
563 Dummermuth S, Fernández-Duque E, Frisenvænge J, Hesseilsøe M, Larson S, Lemaître J-
564 F, McDonald J, Miller DAW, O'Donnell C, Packer C, Raboy BE, Reading CJ, Wapstra E,
565 Weimerskirch H, While GM, Baudisch A, Flatt T, Coulson T, Gaillard, J-M (2018)
566 Diversity of population responses to environmental change. Ecol Lett 22:342-353.
567 https://doi.org/10.1111/ele.13195
568 Dey S, Joshi A (2006) Stability via asynchrony in *Drosophila* metapopulations with low
569 migration rates. Science 312:434-436. https://doi.org/10.1126/science.1125317
570 Díaz S, Settele J, Brondízio ES, Ngo HT, Agard J, Arneth A, Balvanera P, Brauman KA,
571 Butchart SHM, Chan KMA, Garibaldi LA, Ichii K, Liu J, Subramanian SM, Midgley GF,
572 Miloslavich P, Molnár Z, Obura D, Pfaff A, Polasky S, Purvis A, Razzaque J, Reyer B,
573 Roy Chowdhury R, Shin Y-J, Visseren-Hamakers I, Willis KJ, Zayas CN (2019) Pervasive
574 human-driven decline of life on Earth points to the need for transformative change. Science
575 266:eaax3100. https://doi.org/10.1126/science.aax3100
576 Elaydi SN, Sacker RJ (2009) Population models with Allee effect: a new model. J Biol Dynam
577 4:397-408. https://doi.org/10.1080/17513750903377434
578 Estay SA, Lima M, Harrington R (2009) Climate mediated exogenous forcing and synchrony in
579 populations of the oak aphid in the UK. Oikos 118:175-182. https://doi.org/10.1111/j.1600-
580 0706.2008.17043.x

581 Ferguson JM, Ponciano JM (2013) Predicting the process of extinction in experimental
582 microcosms and accounting for interspecific interactions in single-species time series. Ecol
583 Lett 17:251-259. https://doi.org/10.1111/ele.12227
584 Fisher RA (1930) The genetic theory of natural selection. The Clarendon Press, Oxford
585 Fretwell SD (1972) Populations in a seasonal environment. Princeton University Press, Princeton
586 García-Díaz P, Prowser TAA, Anderson DP, Lurgi M, Binny RN, Cassey P (2019) A concise
587 guide to developing and using quantitative models in conservation management. Conserv
588 Sci Practice 1:e11. https://doi.org/10.1111/csp2.11
589 Gelman A, Goodrich B, Gabry J, Vehtari A (2018) R-squared for Bayesian regression models.
590 Am Stat 73:307-309. https://doi.org/10.1080/00031305.2018.1549100
591 Geritz SAH, Kisdi É (2004) On the mechanistic underpinning of discrete-time population models
592 with complex dynamics. J Theor Biol 228:261-269.
593 https://doi.org/10.1016/j.jtbi.2004.01.003
594 Gimona A (1999) Theoretical framework and practical tools for conservation o biodiversity at
595 the landscape scale. *Planning in Ecological Network (PLANECO) Newsletter*, 2: 1-3.
596 Griffen B, Drake J (2008) Effects of habitat quality and size on extinction in experimental
597 populations. Proc R Soc Lond B 275:2251-2256. https://doi.org/10.1098/rspb.2008.0518
598 Hassell MP (1986) Detecting density dependence. Trends Ecol Evol 1:90-93.
599 https://doi.org/10.1016/0169-5347(86)90031-5
600 Hastings A (2014) Temporal scales of resource variability: effects on dynamics of structured
601 populations. Ecol Complex 18:6-9. https://doi.org/10.1016/j.ecocom.2013.08.003
602 Intergovernmental Science-Policy Platform on Biodiversity and Ecosystem Services (IPBES)
603 (2019) Global assessment report on biodiversity and ecosystem services. Díaz S, Settele J,
604 Brondízio ES, Ngo HT, Guèze M, Argard J et al (eds). IPBES Secretariat, Bonn
605 Kilgour RJ, McAdam AG, Betini GS, Norris DR (2018) Experimental evidence that density
606 mediates negative frequency-dependent selection on aggression. J Anim Ecol 87:1091-
607 1101. https://doi.org/10.1111/1365-2656.12813
608 Kilgour RJ, McAdam AG, Norris DR (2020) Carry-over effects of resource competition and
609 social environment on aggression. Behav Ecol 31:140-151.
610 https://doi.org/10.1093/beheco/arz170

611 Kot M, Schaffer WM (1984) The effects of seasonality on discrete models of population growth.
612 Theor Popul Biol 26:340-360. https://doi.org/10.1016/0040-5809(84)90038-8
613 Lande R, Engen S, Sæther B-E (2003) Stochastic population dynamics in ecology and
614 conservation. Oxford University Press, Oxford
615 Leatherbury KN, Travis J (2019) The effects of food level and social density on reproduction in
616 the least killifish, *Heterandria formosa*. Ecol Evol 9:100-110.
617 https://doi.org/10.1002/ece3.4634
618 Liz E (2017) Effects of strength and timing of harvest on seasonal population models: stability
619 switches and catastrophic shifts. Theor Ecol 10:235-244. https://doi.org/10.1007/s12080-
620 016-0325-9
621 Liz E, Ruiz-Herrera A (2016) Potential impact of carry-over effects in the dynamics and
622 management of seasonal populations. PLoS One:e0155579.
623 https://doi.org/10.1371/journal.pone.0155579
624 Ludwig D (1996). The distribution of population survival times. Am Nat 147:506-526.
625 https://doi.org/10.1086/285863
626 May RM (1987) Chaos and the dynamics of biological populations. Proc R Soc Lond A 413:27-
627 44. https://doi.org/10.1098/rspa.1987.0098
628 May RM, Oster GF (1976) Bifurcations and dynamic complexity in simple ecological models.
629 Am Nat 110:573-799. https://doi.org/10.1086/283092
630 Mueller LD, Joshi A (2000). Stability in model populations. Princeton University Press,
631 Princeton
632 Myers RA, Bowen KG, Barrowman NJ (1999) Maximum reproductive rate of fish at low
633 population sizes. Can J Fish Aquat Sci 56:2404-2419. https://doi.org/10.1139/f99-201
634 Norris DR (2005) Carry-over effects and habitat quality in migratory populations. Oikos
635 109:178-186. https://doi.org/10.1111/j.0030-1299.2005.13671.x
636 Norris DR, Taylor CM (2005) Predicting the consequences of carry-over effects for migratory
637 populations. Biol Lett 2:148-151. https://doi.org/10.1098/rsbl.2005.0397
638 Norris K (2004) Managing threatened species: the ecological toolbox, evolutionary theory and
639 declining-population paradigm. J Appl Ecol 41:413-426. https://doi.org/10.1111/j.0021-
640 8901.2004.00910.x

O'Connor CM, Cooke SJ (2015) Ecological carryover effects complicate conservation. Ambio 44:582-591. https://doi.org/10.1007/s13280-015-0630-3

O'Connor CM, Norris DR, Crossin GT, Cooke SJ (2014) Biological carryover effects: linking common concepts and mechanisms in ecology and evolution. Ecosphere 5:1-11. https://doi.org/10.1890/ES13-00388.1

Otso O, Meerson B (2010) Stochastic models of population extinction. Trends Ecol Evol 25:643-652. https://doi.org/10.1016/j.tree.2010.07.009

Pearl R, Reed LJ (1920) On the rate of growth of the population of the United States since 1790 and its mathematical representation. Proc Natl Acad Sci USA 6:275-288. https://doi.org/10.1073/pnas.6.6.275

Pimm SL, Jenkins CN, Abell R, Brooks TM, Gittleman JL, Joppa LN, Raven PH, Roberts CM, Sexton JO (2014) The biodiversity of species and their rates of extinction, distribution, and protection. Science 344:1245752. https://doi.org/10.1126/science.1246752

Ratikainen II, Gill JA, Gunnarsson TG, Sutherland WJ, Kokko H (2007) When density dependence is not instantaneous: theoretical developments and management implications. Ecol Lett 11:184-198. https://doi.org/10.1111/j.1461-0248.2007.01122.x

R Core Team (2020) R: a language and environment for statistical computing. R Foundation for Statistical Computing, Vienna

Ricker WE (1954) Stock and recruitment. J Fish Board Can:559-623. https://doi.org/10.1139/f54-039

Ricker WE (1963) Big effects from small causes: two examples from fish population dynamics. J Fish Board Can 20:257-264. https://doi.org/10.1139/f63-022

Rosenblat S (1980) Population models in a periodically fluctuating environment. J Math Biol 9:23-36. https://doi.org/10.1007/BF00276033

Romero MA, Grandi MF, Koen-Alonso M, Svendsen G, Ocampo Reinaldo M, García NA, Dans SL, González R, Crespo EA (2017) Analysing the natural population growth of a large marine mammal after a depletive harvest. Sci Rep 7:5271. https://doi.org/10.1038/s41598-017-05577-6

Sacker RJ (2007) A note on periodic Ricker maps. J Differ Equ Appl 13:89-92. https://doi.org/10.1080/10236190601008752

671 Sillett TS, Holmes RT (2005). Long-term demographic trends, limiting factors, and the strength
672 of density dependence in a breeding population of a migratory songbird. In: Greenberg R,
673 Marra PP (eds) Birds of two worlds: the ecology and evolution of temperate-tropical
674 migration systems. Smithsonian Institute Press, Washington, D.C.
675 Skellam JG (1967) Seasonal periodicity in theoretical population ecology. Proc 5th Berkley
676 Symp Math Stat Probab 4:179-205.
677 Sokolowski MB, Pereira HS, Hughes K (1997) Evolution of foraging behaviour in *Drosophila*
678 by density-dependent selection. Proc Natl Acad Sci USA 94:7373-7377.
679 https://doi.org/10.1073/pnas.94.14.7373
680 Stephens PA, Sutherland WJ, Freckleton RP (1999) What is the Allee effect? Oikos 87:185-190.
681 https://doi.org/10.2307/3547011
682 Sutherland WJ (1996) Predicting the consequences of habitat loss for migratory populations.
683 Proc R Soc Lond B 263:1325-1327. https://doi.org/10.1098/rspb.1996.0194
684 Turchin P (2003) Complex population dynamics: a theoretical/empirical synthesis. Princeton
685 University Press, Princeton
686 Twombly S, Wang G, Hobbs NT (2007) Composite forces shape population dynamics of
687 copepod crustaceans. Ecology 88:658-670. https://doi.org/10.1890/06-0423
688 Verhulst P-F (1845) Recherches mathématiques sur la loi d'accroissement de la population
689 [French; mathematical researches into the law of population growth increase]. *Nouveaux*
690 *Mémoires de l'Académie Royale des Sciences et Belles-Lettres de Bruxelles* 18:8.
691 White ER, Hasting A (2020) Seasonality in ecology: progress and prospects in theory. Ecol
692 Complex 44:100867. https://doi.org/10.1016/j.ecocom.2020.100867
693 World Wildlife Fund (WWF) (2018) Living planet report – 2018: aiming higher. Grooten M,
694 Almond REA (eds). World Wildlife Fund, Gland, Switzerland
695 Wysham DB, Hastings A (2008) Sudden shifts in ecological systems: intermittency and
696 transients in the coupled Ricker population model. Bull Math Biol 70:1013-1031.
697 https://doi.org/10.1007/s11538-007-9288-8
698

Figure Captions

Figure 1. Population dynamics generated from a bi-seasonal Ricker model with season-specific habitat loss. Each generation is comprised of two counts: non-breeding population abundance (i.e., the number of individuals at the start of the non-breeding period; peaks), and breeding population abundance (i.e., the number of potential breeders at the start of the breeding period; troughs). Replicate populations were simulated under control (no habitat loss conditions) for 20 generations while they grew toward carrying capacity (shaded grey region). In subsequent generations, season-specific habitat loss was simulated at 2%, 5%, 10%, 20%, or 25% per generation (see *Theoretical model simulations* in *Methods*). Sample size = 25 replicates per treatment.

Figure 2. Response of *per capita* reproduction to season-specific habitat loss with varying strengths of density dependence. In each generation, *per capita* reproduction was calculated as the number of offspring divided by the number of breeders. All replicates were simulated under control (no habitat loss conditions) for 20 generations while they grew toward carrying capacity (shaded grey region). In subsequent generations, season-specific habitat loss was simulated at 2%, 5%, 10%, 20%, or 25% per generation (see *Theoretical model simulations* in *Methods*). Sample size = 25 simulations per treatment.

Figure 3. Response of non-breeding survival to season-specific habitat with varying strengths of density dependence. In each generation, non-breeding survival was calculated as the number of individuals at the end of the non-breeding period divided by the number initial non-breeding abundance (i.e., the proportion of individuals who survived through the non-breeding period). All replicates were simulated under control (no habitat loss conditions) for 20 generations while they grew toward carrying capacity (shaded grey region). In subsequent generations, season-specific habitat loss was simulated at 2%, 5%, 10%, 20%, or 25% per generation (see *Theoretical model simulations* in *Methods*). Sample size = 25 simulations per treatment.

Figure 4. Rate of habitat loss, strength of density dependence, and the timing of population collapse with season-specific habitat loss. To explore how the strength of density dependence influences the timing of population collapse, we parameterized our bi-seasonal Ricker model under three different theoretical scenarios of density dependence and using the experimental parameters obtained from our seasonal populations of *Drosophila* (see *Theoretical model simulations* in *Methods*). The time to extinction was calculated as the number of generations of season-specific habitat loss at a particular rate before the populations collapsed, excluding the 20 generations of 'pre-treatment' in which populations were simulated under control conditions.

Figure 5. Effect of changing the strength of (a) non-breeding and (b) breeding density dependence for simulations of 10% non-breeding habitat loss. To explore the effect of density-dependence on time to extinction with non-breeding habitat loss, we systemically varied the strength of density dependence in either the breeding or non-breeding period, while holding density dependence constant in the other period (e.g., by setting breeding density dependence as moderate and vary the strength of non-breeding density dependence; see *Relative strength of density dependence* in *Methods*). Single, deterministic model runs were conducted for each pairwise combination of strengths of breeding and non-breeding density dependence. Extinction time was determined by performing a single iteration of the non-breeding habitat loss model with each combination of breeding and non-breeding strengths of density dependence.

Figures

Figure 1.

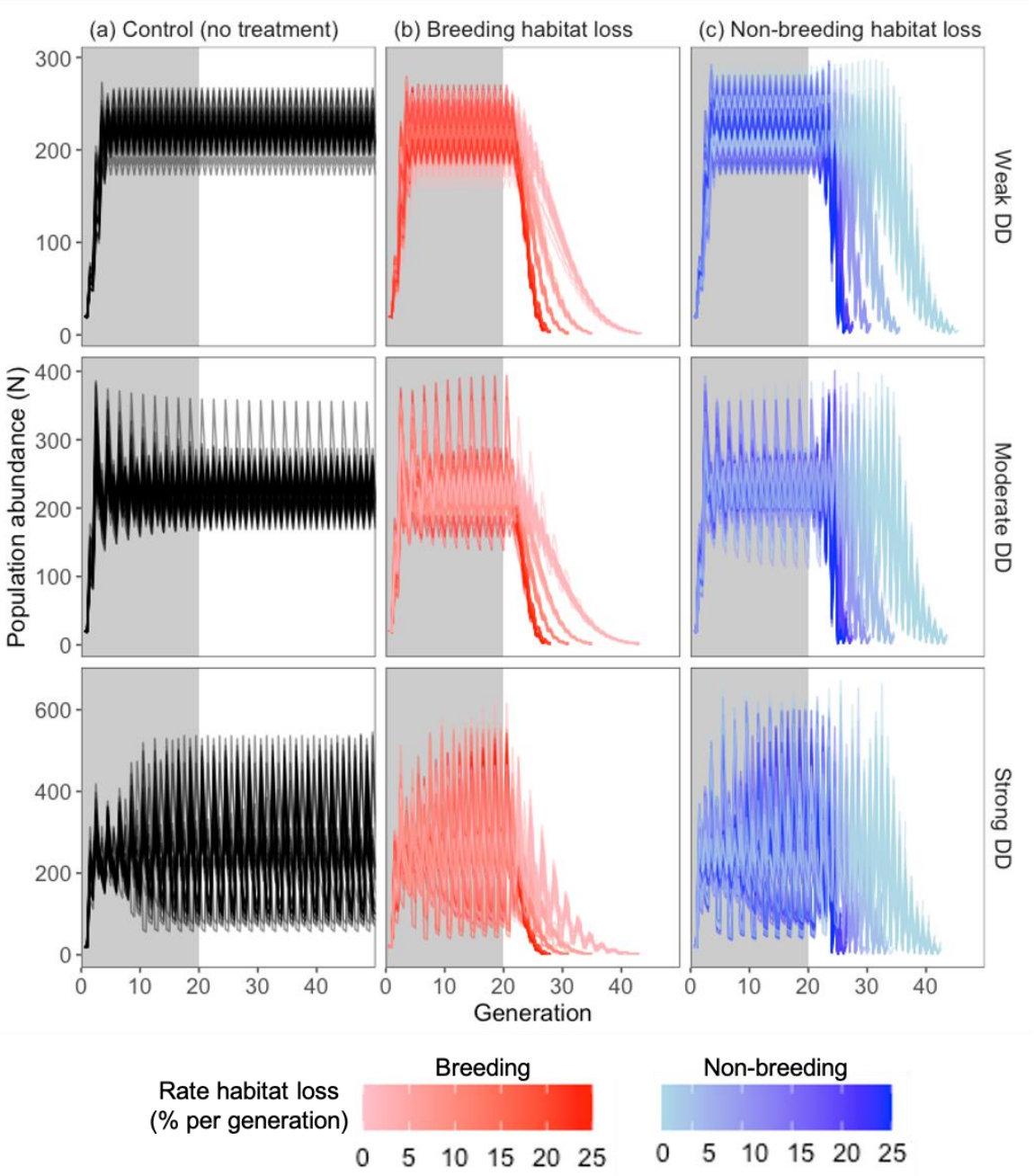

745 Figure 2.

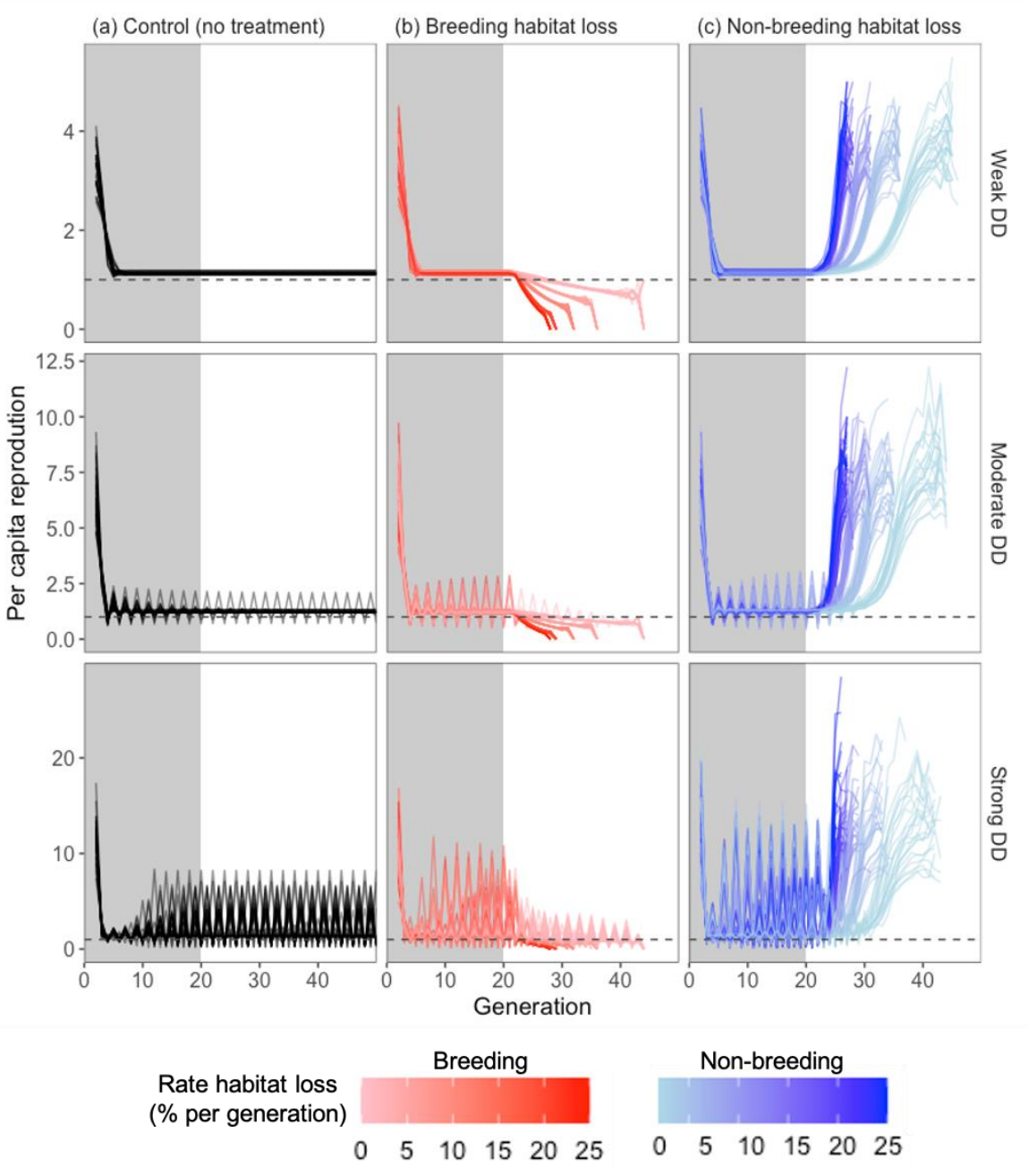

746

747 Figure 3.

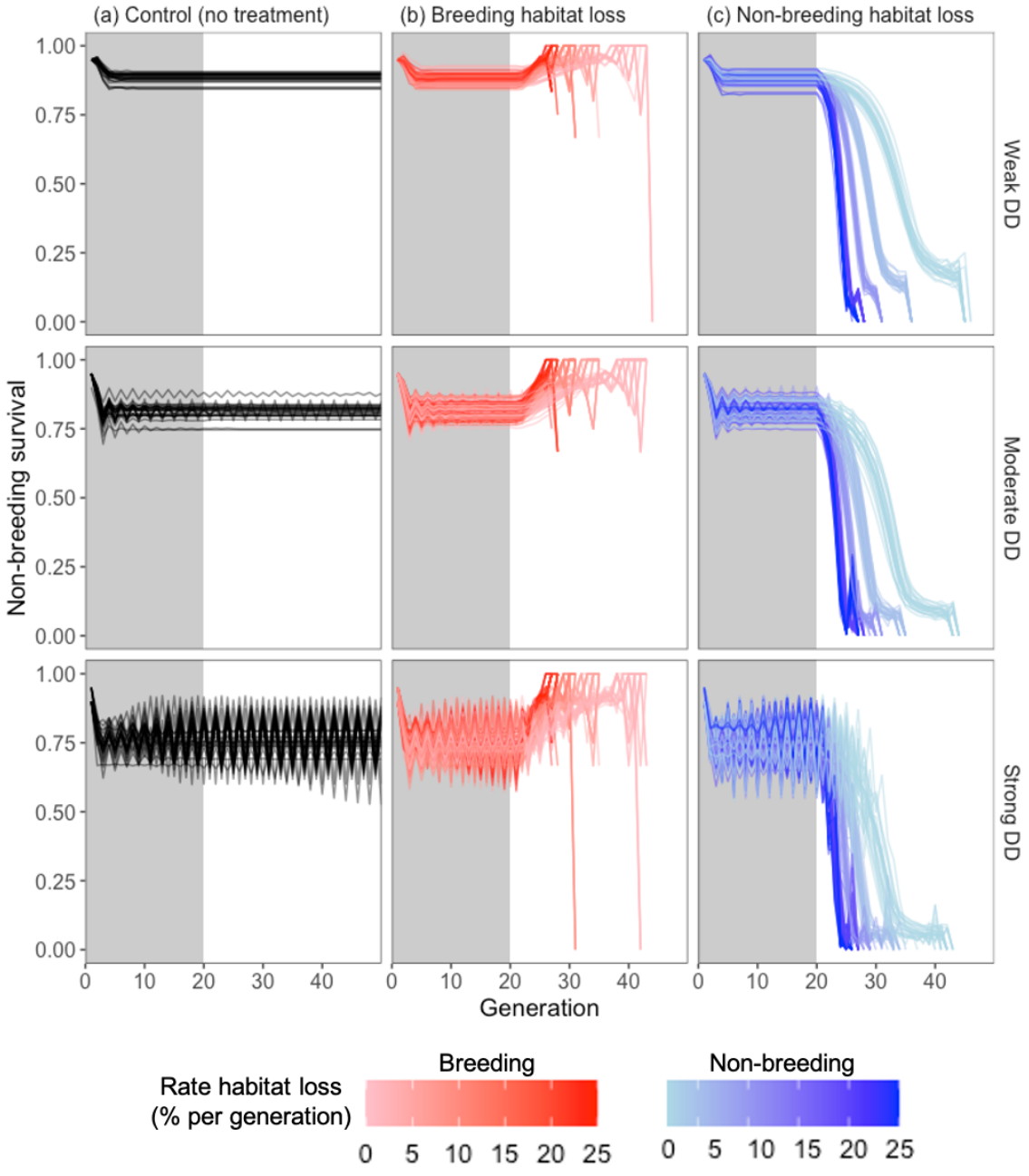

748

749 Figure 4.

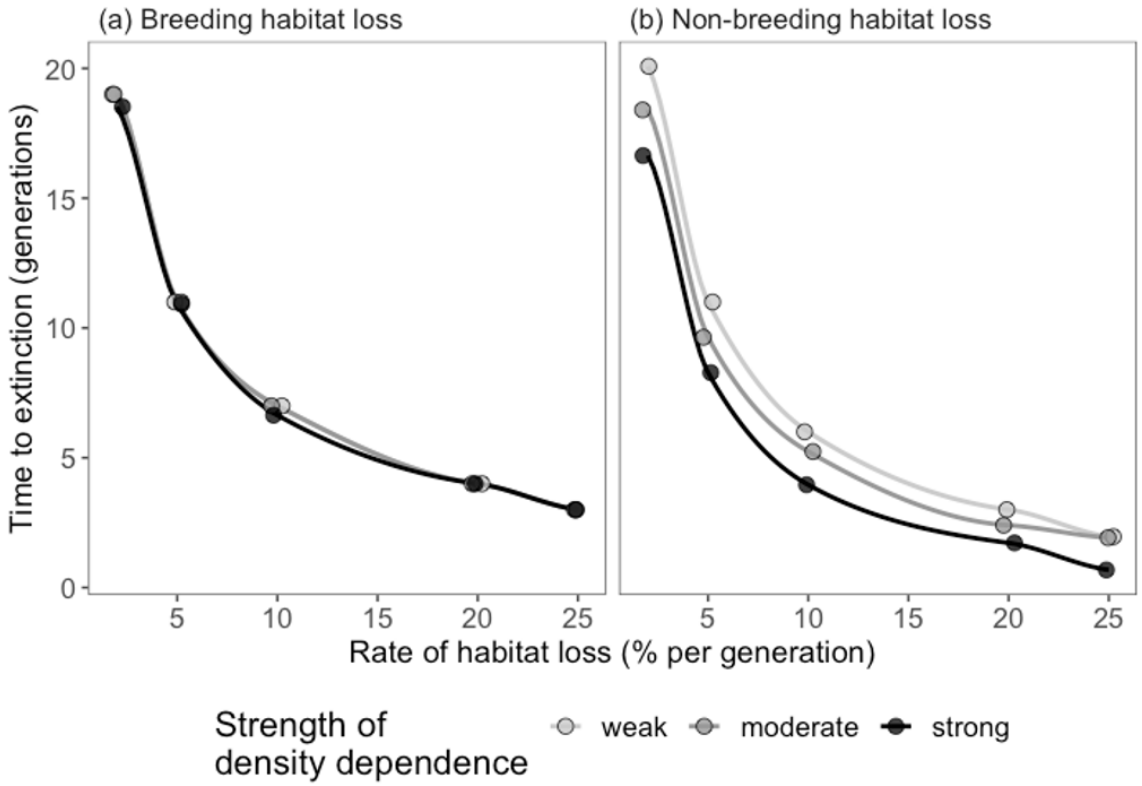

750

751 Figure 5.

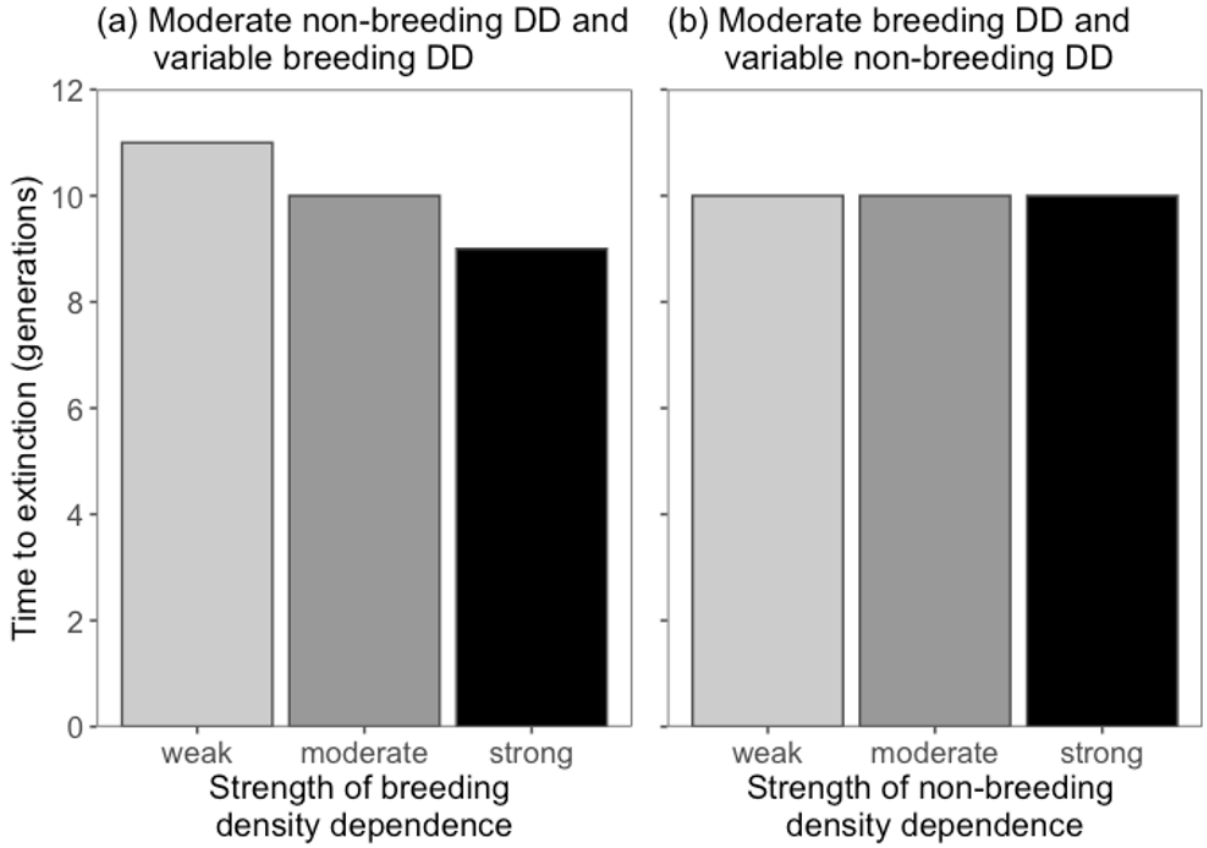

752

Supplementary Information

Supplementary information for: “When habitat is lost matters: patterns of population decline and time to extinction in a seasonal, density-dependent model”

Authors: Joseph B. Burant and D. Ryan Norris

Journal: XXXXX

760 Figurer S1. Breeding population abundance was calculated as the number of potentially breeders
761 at the beginning of the breeding period (i.e., the number of individuals who survived through the
762 previous non-breeding period. All replicates were simulated under control conditions (no habitat
763 loss) for 20 generations prior to the onset of treatment. Sample size = 25 replicates season and
764 rate of habitat loss.

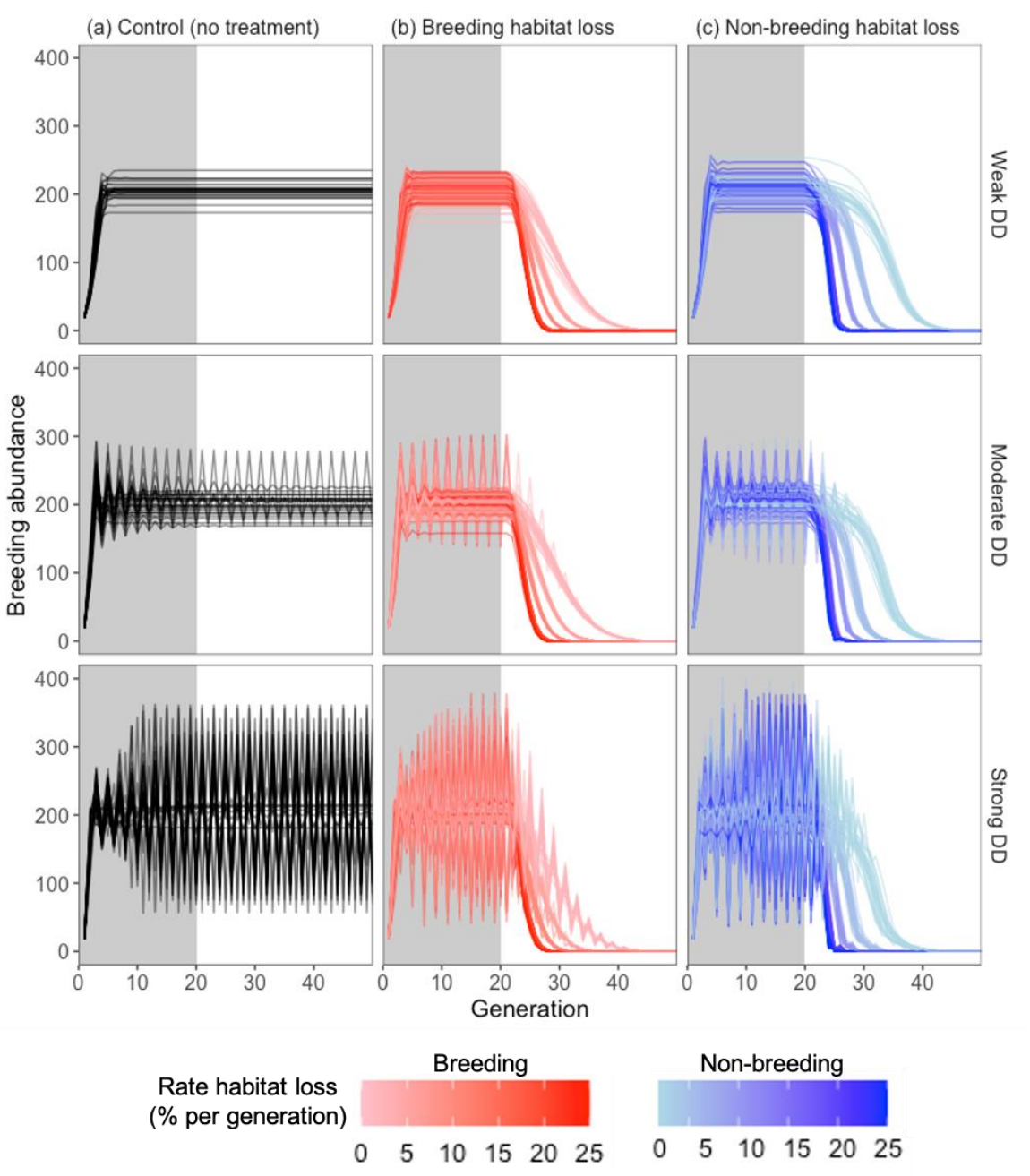

765

Figure S2. Non-breeding population abundance was calculated as the number of individuals at the start of the non-breeding period (i.e., the number of adult offspring produced by the previous generation). All replicates were simulated under control conditions (no habitat loss) for 20 generations prior to the onset of treatment. Sample size = 25 replicates per season and rate of habitat loss.

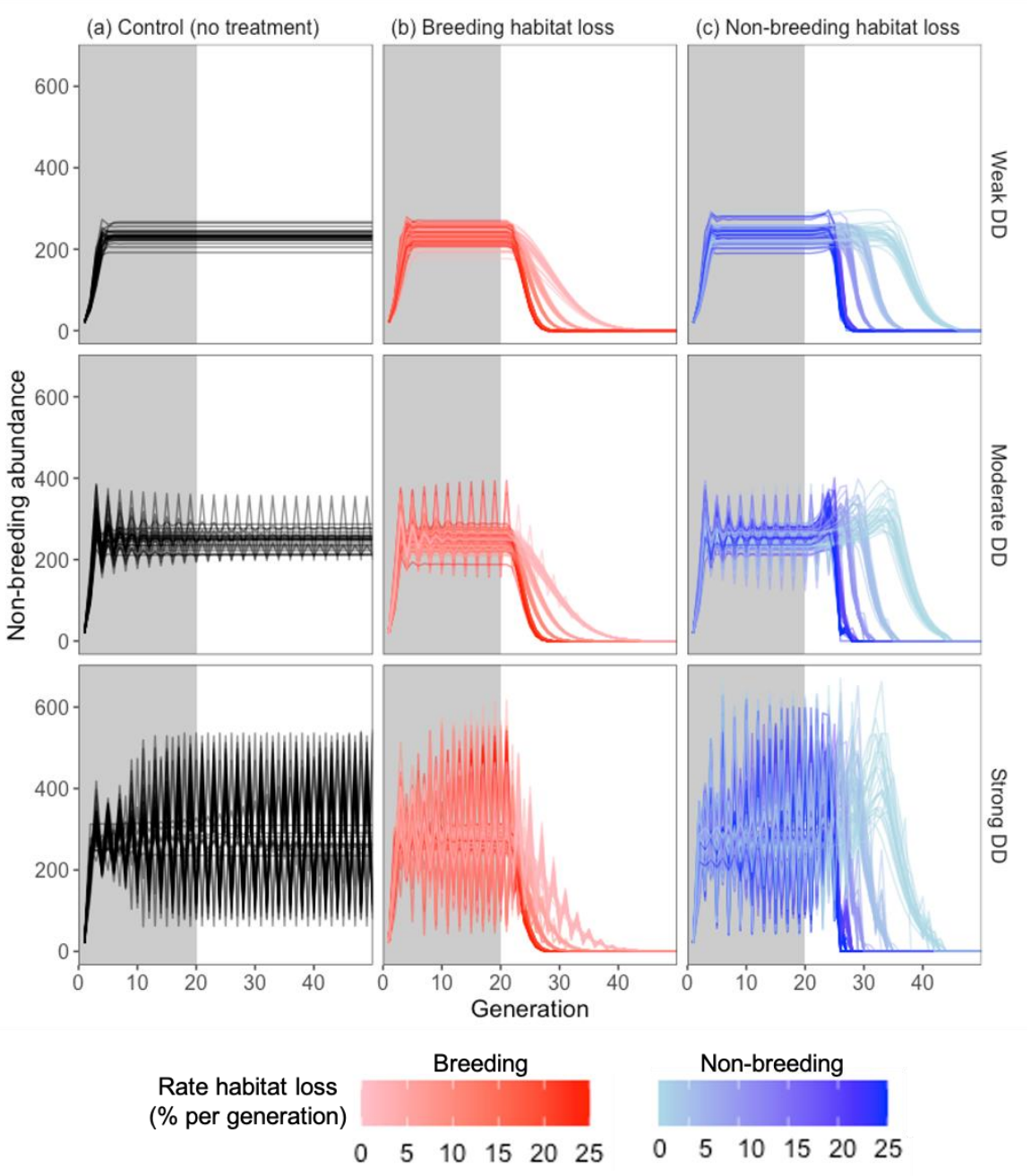

Figure S3. Bi-seasonal and season-specific population abundances from models parameterized with empirical values from seasonal populations of *Drosophila melanogaster* (Part 1). All replicates were simulated under control (no habitat loss conditions) for 20 generations while they grew toward carrying capacity (shaded grey region). In subsequent generations, season-specific habitat loss was simulated at 2%, 5%, 10%, 20%, or 25% per generation (see *Theoretical model simulations* in *Methods*). Sample size = 25 replicates per season and rate of habitat loss.

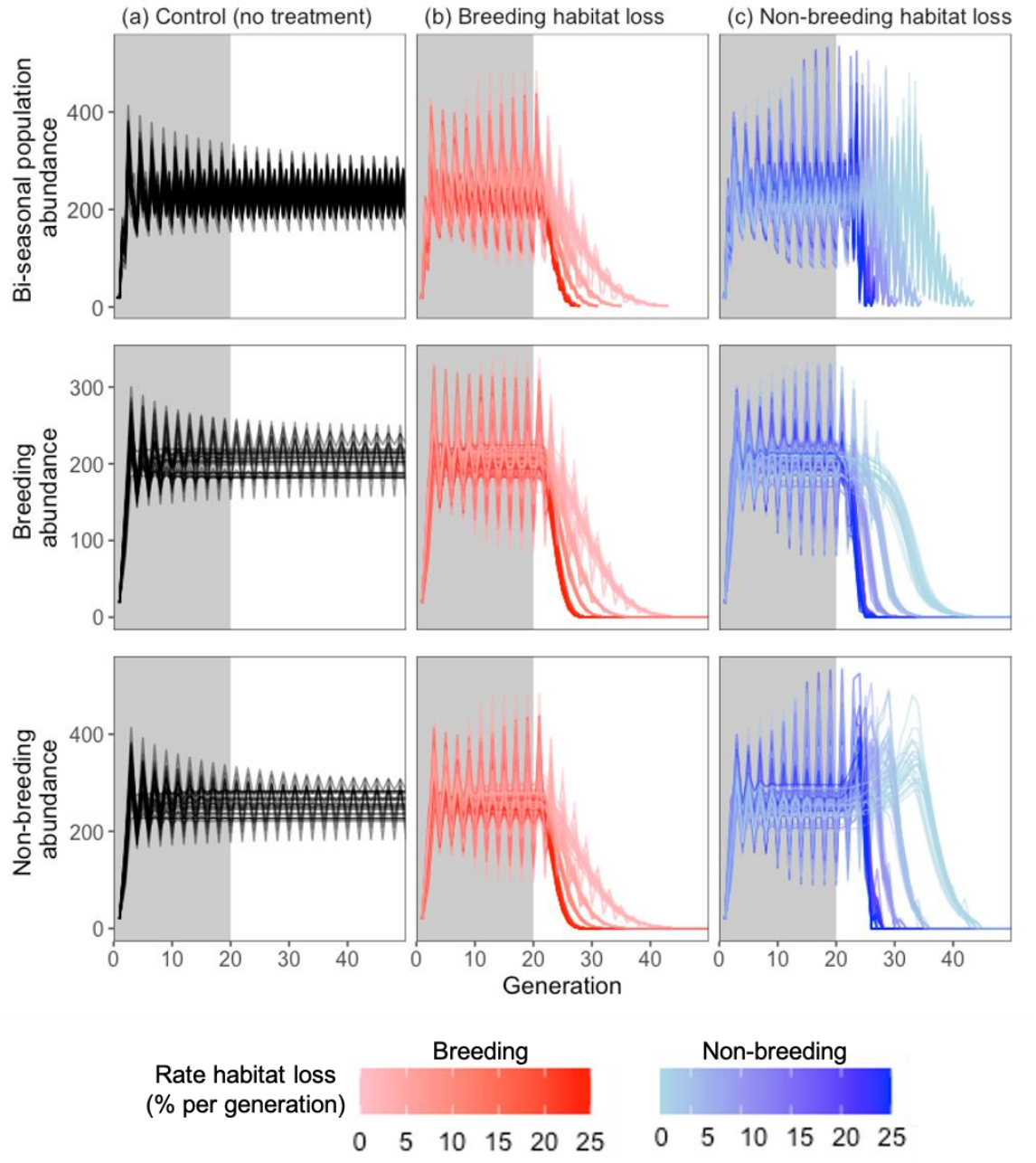

Figure S4. *Per capita* reproductive output (breeding period) and survival (non-breeding period) from model simulations of chronic habitat loss parameterized with empirical values from seasonal populations of *Drosophila melanogaster* (Part 2). In replicate simulations, populations were exposed to (a) no habitat loss (control), (b) breeding habitat loss, or (c) non-breeding habitat loss. In each generation, *per capita* reproduction was calculated as the number of offspring divided by the number of breeders, and non-breeding survival was calculated as the number of individuals at the end of the non-breeding period divided by initial non-breeding population size. All replicates were simulated under control (no habitat loss conditions) for 20 generations while they grew toward carrying capacity (shaded grey region). In subsequent generations, season-specific habitat loss was simulated at 2%, 5%, 10%, 20%, or 25% per generation (see *Theoretical model simulations* in *Methods*). (d, e) *per capita* reproduction as a function of breeding population size. (f, g) non-breeding survival as a function of non-breeding population size. In general, for d-g, seasonal population abundances shifted from right (high) to left (low) along the x-axis as habitat loss progressed (see Fig. 3, Fig. 4 in main text). Number of observations: $n_{reproduction(B\ loss)} = 1488$; $n_{reproduction(NB\ loss)} = 1311$; $n_{survival(B\ loss)} = 1408$; $n_{survival(NB\ loss)} = 1500$. Sample size (N) = 25 simulations per treatment.

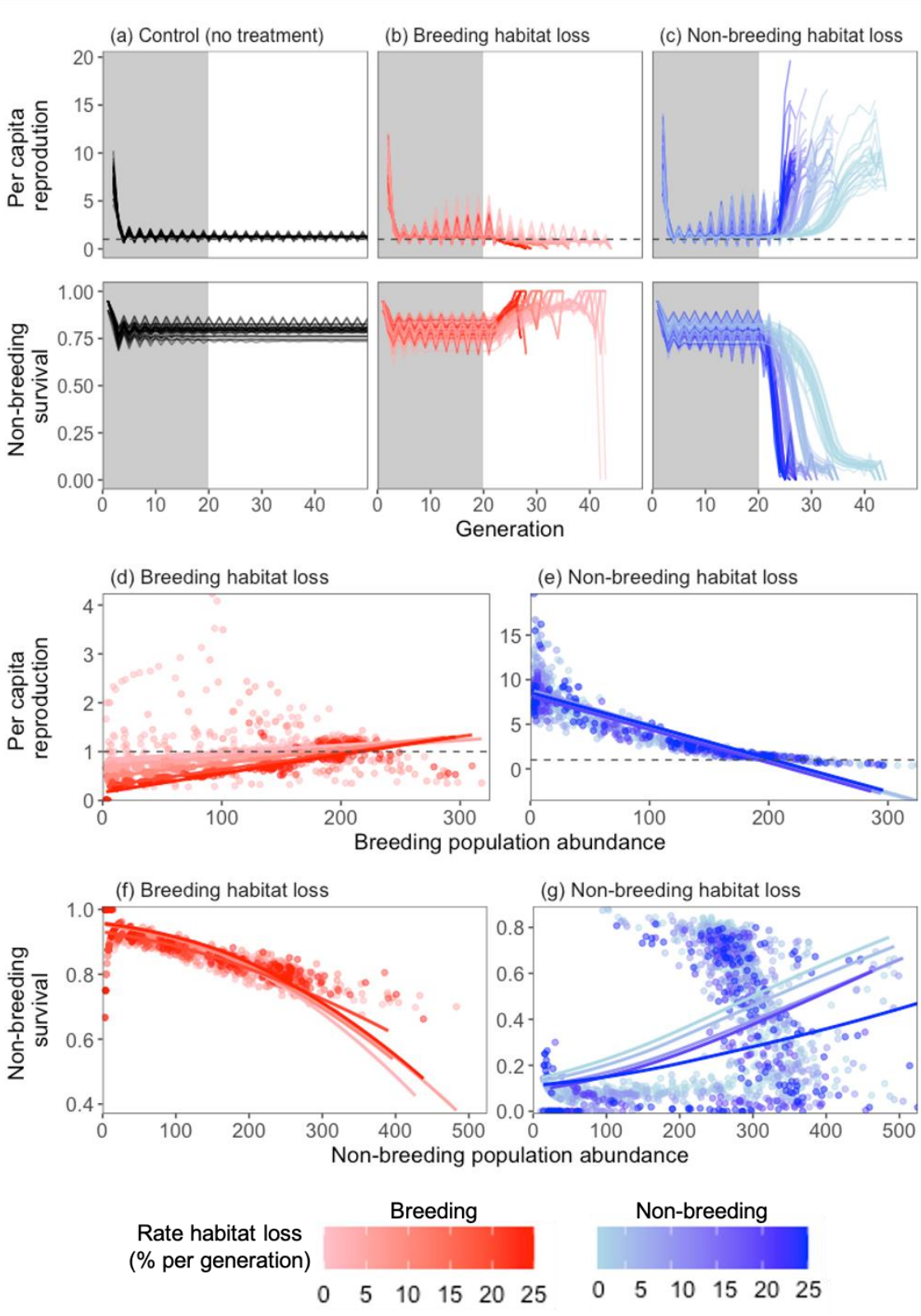
(a) Control (no treatment)
(b) Breeding habitat loss
(c) Non-breeding habitat loss
Per capita reprodution
Non-breeding survival
Generation
(d) Breeding habitat loss
(e) Non-breeding habitat loss
Per capita reproduction
Breeding population abundance
(f) Breeding habitat loss
(g) Non-breeding habitat loss
Non-breeding survival
Non-breeding population abundance
Rate habitat loss (% per generation)
Breeding
Non-breeding
0 5 10 15 20 25
0 5 10 15 20 25

795

Statistical analysis for Fig. S4

We used simulations from bi-seasonal Ricker model parameterized using information empirically-derived from seasonal *Drosophila* populations (see above; Betini et al. 2013a) to investigate how the seasonal vital rates (reproduction and non-breeding survival) changed in response to changes in seasonal population abundance with habitat loss. To do this, we used four separate mixed effects models (Bolker et al. 2009): two models for each vital rate (one for breeding habitat loss treatments and one for non-breeding habitat loss treatments). All statistical models were fitted in a Bayesian framework (Ellison 2004). In each model, the seasonal vital rate of interest was regressed against the two-way interaction between the corresponding abundance value (integer) and the rate of habitat loss treatment (5-level factor: 2, 5, 10, 20, 25). Simulation number was fitted as a random effect, with a random slope term included for the rate of habitat loss. Because we were interested in modelling the effects of habitat loss, we only included data from the treatment period (after 20 generations of control conditions; see *Theoretical model simulations* above).

Per capita reproduction was modelled as a function of breeding population abundance with linear mixed effects models (LMM; family = Gaussian, link-function = identity). Non-breeding survival, a proportion ranging [0, 1], was modelled as a function of non-breeding population abundance with generalized linear mixed effects models (GLMM; family = Beta, link-function = logit; Ferrari and Cribari-Neto 2004). Importantly, the beta distribution cannot be used to model zeroes and ones, and so does not include the maximum bounds of the data range (Duoma and Weedon 2019). To account for this, non-breeding survival for populations losing non-breeding habitat (range = [0, 1)) was modelled as (survival + 0.0001) to account for zeroes in the dataset. In contrast, populations losing breeding habitat reached 100% non-breeding survival at low non-breeding densities, and so all values were modelled as (survival – 0.0001).

We specified the statistical models using flat priors, with each model consisting of four chains of 5,000 iterations, a burn-in period of 1,000 iterations per chain, and post-sampling thinning to every fourth iteration (n_{chain} = 1,000 iterations; n_{model} = 4,000 iterations). Model convergence was confirmed by consulting $\hat{R}$ values (equal to 1 at convergence), as well as inspecting the posterior distributions of fitted values and caterpillar plots (Bürkner 2017). Estimates of the effect size of predictor variables were taken from the posterior distributions of the model parameters, with 95 percent credible intervals (C.I.) around the means (β) made based

on the 4,000 samples from each statistical model (Cumming and Finch 2005). Model fit was estimated using Bayesian R^2 as the proportion of variance explained (Gelman et al. 2018).

Summary of results in Fig. S4

Simulations from our theoretical models produce clear evidence for an impact of sequential density dependence on the population vital rates: *per capita* reproduction and non-breeding survival. When breeding habitat was lost, *per capita* reproduction declined as habitat loss progressed. As a consequence, there was strong evidence for a positive relationship between breeding population abundance (i.e., the number of potential breeders) and *per capita* reproductive output (breeding habitat loss: $R^2_{r_b \sim N_b}$ = 0.377, 95% C.I. = (0.344, 0.408)), such that as populations lost breeding habitat and the number of breeding individuals declined, *per capita* reproductive output also declined (Table S1). The strength of the relationship between breeding abundance and *per capita* reproduction increased (and so the intercept got smaller) with the rate of breeding habitat loss treatment (Table S1). By contrast, non-breeding habitat loss generated an increase in *per capita* reproduction as habitat loss progressed, since fewer potential breeders survived the previous non-breeding period. We found strong evidence for a negative relationship between *per capita* reproduction and breeding abundance for non-breeding habitat loss treatments (non-breeding habitat loss: $R^2_{r_b \sim N_b}$ = 0.881, 95% C.I. = (0.875, 0.885)), such that as simulations lost non-breeding habitat and the number of potential breeders declined, *per capita* reproductive output increased (Table S1). The strength of the relationship between breeding abundance and *per capita* reproduction decreased (and so the intercept got smaller) with the rate of non-breeding habitat loss treatment (Table S1).

Non-breeding survival increased with breeding habitat loss treatments, since fewer offspring were produced by the preceding generation and so individuals experienced reduced density dependence in the non-breeding period. As a result, we found strong evidence for a negative relationship between non-breeding population abundance and non-breeding survival (breeding habitat loss: $R^2_{r_{nb} \sim N_{nb}}$ = 0.726, 95% C.I. = (0.720, 0.732)), such that as breeding habitat loss progressed and so initial non-breeding abundance decreased, non-breeding survival increased (Table S2). With non-breeding habitat loss, non-breeding survival decreased as treatment progressed with relatively dampened changes in non-breeding population abundance until later generations, due to density-dependent reproduction. For non-breeding treatments,

there was a positive relationship between non-breeding abundance and non-breeding survival (non-breeding habitat loss: $R^2_{r_{nb} \sim N_{nb}}$ = 0.210, 95% C.I. = (0.188, 0.234); Table S2), although this relationship was highly nonlinear.

References for analyses presented in Fig. S4

Bolker BM, Brooks ME, Clark CJ, Geange SW, Poulson JR, Stevens MHH, White J-SS (2009) Generalized linear mixed models: a practical guide for ecology and evolution. Trends Ecol Evol 24:127-135. https://doi.org/10.1016/j.tree.2008.10.008

Bürkner PC (2017) brms: An R package for Bayesian multilevel models using Stan. J Stat Softw 80:1-28. https://doi.org/10.18637/jss.v080.i01

Cumming G, Finch S (2005) Inference by eye: confidence intervals and how to read pictures of data. Am Psychol 60:170-180. https://doi.org/10.1037/0003-066x.60.2.170

Douma JC, Weedon JT (2019) Analysing continuous proportions in ecology and evolution: a practical introduction to beta and Dirichlet regression. Methods Ecol Evol 10:1412-1430. https://doi.org/10.1111/2041-210X.13234

Ellison AM (2004) Bayesian inference in ecology. Ecol Lett 7:509-520. https://doi.org/10.1111/j.1461-0248.2004.00603.x

Ferrari S, Cribari-Neto F (2004) Beta regression for modelling rates and proportions. J Appl Stat 31:799-815. https://doi.org/10.1080/0266476042000214501

Table S1. Effect size estimates from models of *per capita* reproduction. Two univariate linear mixed effects models were used to test the influence of breeding population abundance (N_b) on changes in *per capita* reproduction (r_b). Separate statistical models were fitted for the results from simulations of the impacts of breeding and non-breeding habitat loss on the relationship between population vital rates (*per capita* reproduction; non-breeding survival) and the corresponding abundance measure (breeding; non-breeding) for models parameterized with empirical values from seasonal populations of *Drosophila melanogaster* (see *Statistical analysis*). Effect size estimates (β) and 95% credible intervals (C.I.) were taken from the posterior distribution of model parameters.

	Breeding habitat loss			**Non-breeding habitat loss**		
Fixed effect	Estimate (β)	Lower 95% C.I.	Upper 95% C.I.	Estimate (β)	Lower 95% C.I.	Upper 95% CI
(Intercept)	0.839	0.792	0.887	8.41	8.07	8.77
Count	0.002	0.001	0.002	-0.037	-0.039	-0.036
Treatment (B05)	-0.132	-0.204	-0.059	0.234	-0.353	0.827
Treatment (B10)	-0.371	-0.451	-0.290	0.507	-0.081	1.08
Treatment (B20)	-0.549	-0.642	-0.453	-0.173	-0.744	0.399
Treatment (B25)	-0.673	-0.763	-0.582	0.234	-0.473	0.932
Count:B05	3×10^{-4}	-3×10^{-4}	0.001	-3×10^{-4}	-0.002	0.002
Count:B10	0.001	0.001	0.002	-0.003	-0.005	-2×10^{-4}
Count:B20	0.002	0.001	0.003	-0.001	-0.003	0.002
Count:B25	0.002	0.002	0.003	-1×10^{-4}	-0.003	0.003
Random effect	Estimate (σ)	Lower 95% C.I.	Upper 95% C.I.	Estimate (σ)	Lower 95% C.I.	Upper 95% CI
sd(Intercept)	0.053	0.022	0.080	0.772	0.572	1.01
sd(B05)	0.035	0.001	0.099	0.724	0.066	1.56
sd(B10)	0.032	0.001	0.086	0.628	0.034	1.52
sd(B20)	0.033	0.001	0.093	0.417	0.015	1.19
sd(B25)	0.033	0.001	0.094	0.880	0.106	1.76
Family-specific	Estimate (σ)	Lower 95% C.I.	Upper 95% C.I.	Estimate (σ)	Lower 95% C.I.	Upper 95% CI
Sigma (σ)	0.322	0.310	0.334	1.16	1.12	1.21

884

Table S2. Effect size estimates from models of non-breeding survival. Two univariate linear mixed effects models were used to test the influence of non-breeding population abundance (N_{nb}) on changes in non-breeding survival (r_{nb}).). Separate statistical models were fitted for the results from simulations of the impacts of breeding and non-breeding habitat loss on the relationship between population vital rates (*per capita* reproduction; non-breeding survival) and the corresponding abundance measure (breeding; non-breeding) for models parameterized with empirical values from seasonal populations of *Drosophila melanogaster* (see *Statistical analysis*). Effect size estimates (β) and 95% credible intervals (C.I.) were taken from the posterior distribution of model parameters. To be interpreted on the scale of the input data (proportions; (0, 1)), estimates of the intercept for each rate of habitat loss must be back-transformed from beta regression estimates using inverse-logit function: $logit^{-1}(n) = e^n/(1 + e^n)$ (Douma and Weedon 2019).

	Breeding habitat loss			**Non-breeding habitat loss**		
Fixed effect	Estimate (β)	Lower 95% C.I.	Upper 95% C.I.	Estimate (β)	Lower 95% C.I.	Upper 95% C.I.
(Intercept)	3.14	3.03	3.24	-1.84	-2.03	-1.64
Count	-0.008	-0.009	-0.008	0.006	0.005	0.007
Treatment (B05)	-0.010	-0.177	0.154	-0.146	-0.435	0.154
Treatment (B10)	-0.095	-0.285	0.092	-0.340	-0.691	-0.005
Treatment (B20)	-0.521	-0.723	-0.319	-0.494	-0.879	-0.128
Treatment (B25)	-0.020	-0.228	0.187	-0.287	-0.710	0.114
Count:B05	0.001	-3×10^{-4}	0.001	-1×10^{-4}	-0.001	0.001
Count:B10	0.001	-4×10^{-4}	0.002	-3×10^{-4}	-0.002	0.001
Count:B20	0.003	0.001	0.004	-1×10^{-4}	-0.002	0.002
Count:B25	0.001	-4×10^{-4}	0.002	-0.002	-0.004	-0.001
Random effect	Estimate (σ)	Lower 95% C.I.	Upper 95% C.I.	Estimate (σ)	Lower 95% C.I.	Upper 95% CI
sd(Intercept)	0.065	0.004	0.146	0.095	0.004	0.260
sd(B05)	0.108	0.006	0.254	0.094	0.004	0.275
sd(B10)	0.120	0.006	0.283	0.089	0.004	0.260
sd(B20)	0.124	0.006	0.297	0.106	0.004	0.304
sd(B25)	0.090	0.004	0.247	0.095	0.004	0.260
Family-specific	Estimate (φ)	Lower 95% C.I.	Upper 95% C.I.	Estimate (φ)	Lower 95% C.I.	Upper 95% CI
Phi (φ)	15.82	14.63	17.09	2.18	2.04	2.33

897